#### **CONFERENCE PRE-PRINT**

# INVESTIGATION OF PLASMA PARAMETERS IN SAWTOOTH OSCILLATION BY ABSOLUTE INTENSITY OF SOFT X-RAY EMISSION IN JT-60SA INTEGRATED COMMISSIONING PHASE

# R. SANO,

Naka Institute for Fusion Science and Technology, National Institutes for Quantum and Radiological Science and Technology

Naka, Ibaraki, Japan

Email: sano.ryuichi@qst.go.jp

#### H. HOMMA

Naka Institute for Fusion Science and Technology, National Institutes for Quantum and Radiological Science and Technology

Naka, Ibaraki, Japan

#### M. TAKECHI

Naka Institute for Fusion Science and Technology, National Institutes for Quantum and Radiological Science and Technology

Naka, Ibaraki, Japan

# T. NAKANO

Naka Institute for Fusion Science and Technology, National Institutes for Quantum and Radiological Science and Technology

Naka, Ibaraki, Japan

# Abstract

An electron temperature profile with 1 keV at the plasma centre and its sawtooth oscillation were evaluated from the power spectrum of bremsstrahlung by a soft x-ray diagnostic system in JT-60SA integrated commissioning phase. The evaluation indicates that the observed opposite phase oscillations between high-energy and low-energy bremsstrahlung emissions in soft x-ray signals are due to opposite changes in the electron temperature and density or effective charge. From the absolute intensity of different energy bremsstrahlung emission, it was indicated at sawtooth crashes that the electron temperature decreased while the electron density and/or effective charge increased, respectively. Changes in the profile of products of the electron density and the effective charge indicated a possible inflow of electrons and/or impurities across the inversion radius.

# 1. INTRODUCTION

MHD (magnetohydrodynamic) phenomena, such as sawtooth oscillation, can degrade the performance of magnetically confined plasmas and can lead to disruptive plasma events. The sawtooth oscillation was observed on soft x-ray emission and electron temperature in many plasma devices, such as JT-60U [1], LHD[2], and JET[3]. From the experimental data, which show the electron temperature and density decrease at the plasma centre in the sawtooth crash [4] and theoretical evaluations, the sawtooth oscillation is basically understanded as particle ejection from inside of the surface of q=1 by sawtooth crash. On the other hand, the increase of local or line integrated electron density at the plasma centre by the sawtooth crash is also reported at TCV [5] and W-7X[6] with ECH heating. To understand the sawtooth oscillation, the transient evolution of profiles of plasma parameters should be investigated. However, because of difficulties of fast diagnostics for the profile of the electron density, the evolution of the electron density during the sawtooth oscillation is not commonly evaluated.

An x-ray photodiode array is widely used to measure soft x-ray emission from the core plasma. Because of the fast time response of the x-ray photodiode, the x-ray photodiode array is widely used to measure the sawtooth oscillation. In the x-ray photo diode array, line integrated soft x-ray emission power density along sight line is detected. From the line integrated emission, a profile of local emission power density can be reconstructed using tomographic reconstruction techniques, such as Abel inversion [7]. In plasma devices which have carbon walls, soft x-ray emission is mainly emitted from electron as bremsstrahlung. Because the power spectrum of

bremsstrahlung strongly depends on the electron temperature and density, the spatial profiles of the electron temperature and density can be evaluated from the profile of reconstructed soft x-ray emission. However, the x-ray photodiode array is mainly used as a qualitative measurement without evaluation of absolute emission intensity. The measurement of the plasma parameters using the x-ray photodiode array is not widely applied.

In this study, the evolution of spatial profiles of plasma parameters during the sawtooth oscillation is investigated by the soft x-ray diagnostic system in JT-60SA integrated commissioning phase.

# 2. EXPERIMENTAL

In JT-60SA, a soft x-ray diagnostic system with two photodiode arrays, each of which were equipped with Be filters with different thicknesses, which are 7 and 50  $\mu$ m, to measure soft x-ray intensity at different energies, was installed [8]. These filter thicknesses were determined to filter out line emissions from light impurities, such as C and O, which were expected in JT-60SA integrated commissioning phase. Figure 1 shows the field of view of the soft x-ray diagnostic system. Because the soft x-ray diagnostics system views the lower half of plasma with upper null configurations, the local soft x-ray emission power density in core plasma can be obtained with reconstruction methods, such as Abel inversion [7].

The local emission power density which passes through the Be filter having  $n-\mu m$  thickness,  $S_{Be_n}$ , is expressed as

$$S_{Be_n} = \int B_{Be_n}(v) \in_{v}^{ff} dv \ [Wm^{-3}], \ (1)$$

where  $B_{Be\_n}$  is the transmittance of a Be filter having n- $\mu$ m thickness,  $\in_{\nu}^{ff}$  is the power spectrum of the emission power density of bremsstrahlung. With the assumption that electron velocity distribution is Maxwellian and the Gaunt factor for  $h\nu \approx T_e$  is applied, the power spectrum is expressed as follows

$$\epsilon_{\nu}^{\text{ff}} = 6.8 \times 10^{-51} \frac{Z_{\text{eff}} n_e^2}{\sqrt{T_e/\text{k}}} e^{\frac{-h\nu}{T_e}} \left(\frac{h\nu}{T_e}\right)^{-0.4} [\text{Wm}^{-3} \text{Hz}^{-1}], \qquad (2)$$

Where  $Z_{eff}$  is the effective charge,  $T_e$  is the electron temperature,  $n_e$  is the electron density, k is the Boltzmann

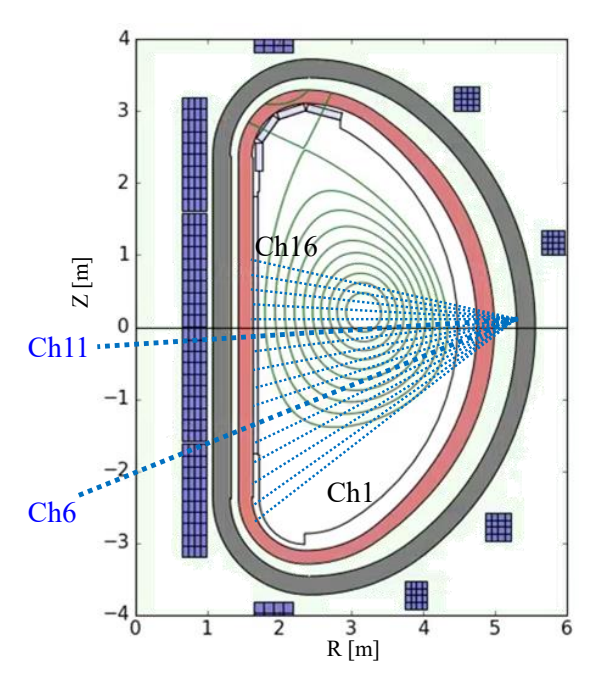


Figure 1 Field of view of the soft x-ray diagnostic system in JT-60SA.

constant and v is the frequency of photon, and h is the Planck constant. From the reconstructed local emission power density profile with two different energy ranges by Be filters, which have 7 and 50 µm thicknesses, the power spectrum of bremsstrahlung at each location can be obtained by "two filters method" [9]. From the power spectrum, the electron temperature and product of electron density and square root of effective charge could be evaluated on the assumption that bremsstrahlung dominated soft x-ray emissions. With this analysis, the profiles of  $T_e$  and  $n_e \sqrt{Z_{eff}}$  in the core plasma can be evaluated for each time slice. To reduce the influence of photon shot noise and background noise on the signal of the soft x-ray diagnostic system, an averaging with 100 time slices was performed on 100 kHz sampled data in the following sections. Therefore, data of the soft x-ray diagnostic system is treated as 1 kHz sampled data. Additionally, the soft x-ray diagnostic system measuring low energy (1 - 8 keV) and high energy (2 - 8 keV) soft x-ray with 7 and 50 μm Be filters are

written as SXR07 and SXR50 in the following sections.

In the campaign of the integrated commissioning of JT-60SA, two types of sawtooth oscillations were observed. One was off-axis sawtooth, which was obtained with ECH injection during ramp up phase of the plasma current. The other type of the sawtooth oscillation was core sawtooth, which peaked at the centre of the plasma. The core sawtooth was mainly observed during the flat top or ramp down phase of the plasma current. The oscillation intensities during the off-axis sawtooth are about 10 - 20% and 20 - 30% of the measured emission power density by SXR07 and SXR50, respectively. On the other hand, the oscillation intensities during the core sawtooth are less than 3% and 6 %, respectively. Both oscillation intensities are evaluated along the sightline views the peak of sawtooth oscillation.

Figure 2 shows time traces of photocurrent of SXR07 and SXR50 during a discharge having the both types of sawtooth oscillation. The photocurrent corresponds to line integrated soft x-ray emission along each sightline. At 2.5-3.0 s, an off-axis sawtooth is observed on channel 6 which views about  $\rho=0.6$ . The oscillation intensities of SXR07 and SXR50 are about 13% and 25%, respectively. The ratio of SXR50 and SXR07 is less than 0.05. It indicates that the electron temperature at the peak of the off-axis sawtooth is less than the limit (150 eV) of the evaluation of the electron temperature by the soft x-ray diagnostic system. From 7.0 s, a core sawtooth is observed on channel 11 which views the centre of plasma ( $\rho=0.0$ ). The oscillation intensities of SXR07 and SXR50 are about 3% and 4%, respectively. The ratio of SXR50 and SXR07 is about 0.32, which indicates that the electron temperature at the peak of the core sawtooth is about 850 eV. The low and high energy range soft x-ray show oscillations in the opposite direction during the core sawtooth along the same sightline. The oscillations of opposite direction cannot be explained with only the electron temperature oscillation.

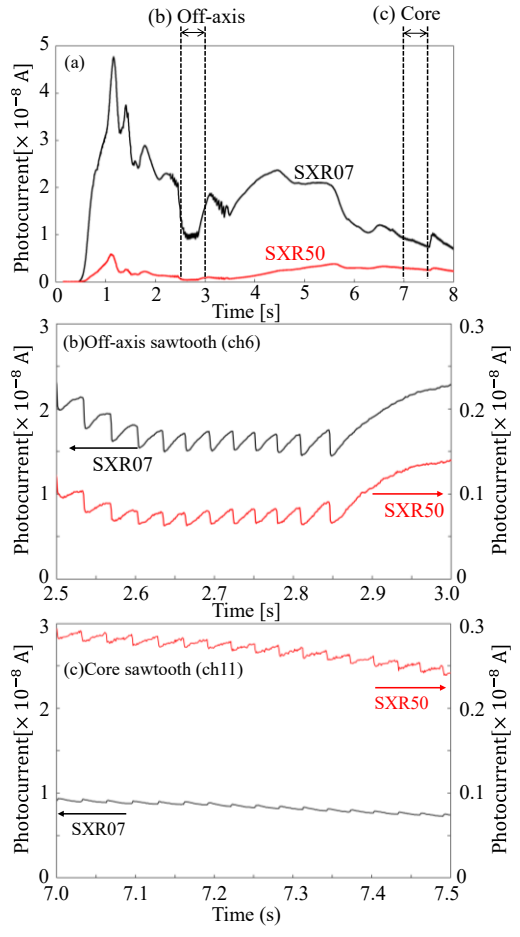


Figure 2 Time traces of photocurrent of (black)SXR07 and (red)SXR50 during (a) the whole discharge, (b)off-axis sawtooth, and (c) core sawtooth. (a) and (c) show signal along channel 11. (b) shows signal along channel 6. (shot #101025)

In the campaign of the integrated commissioning of JT-60SA, 19 discharges having sawtooth oscillation were obtained. The core, off-axis, and both types sawtooth were observed in 11, 5, and 3 discharges out of the 19 discharges. The off-axis sawtooth is out of the scope of this manuscript because the electron temperature of the peak of the sawtooth oscillation is difficult to evaluate by the soft x-ray diagnostic system due to a low signal-to-noise ratio.

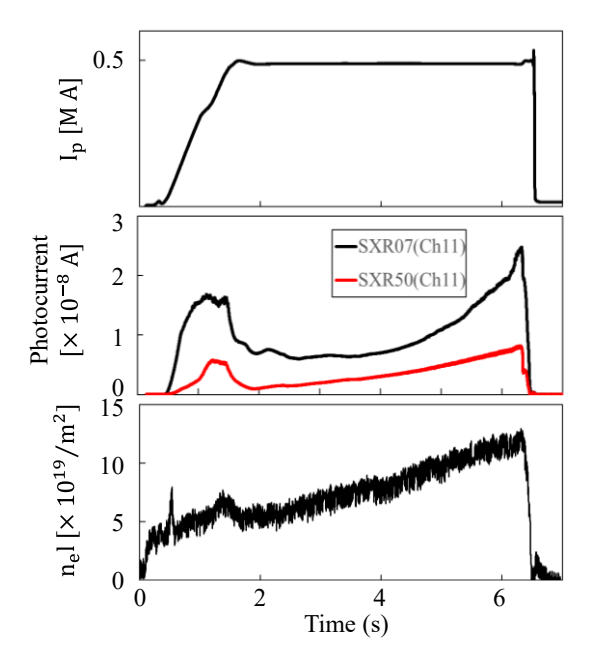


Figure 3 Time traces of (upper) plasma current, (middle) photocurrent of SXR07 and SXR50, and (lower) line density. (shot #101008).

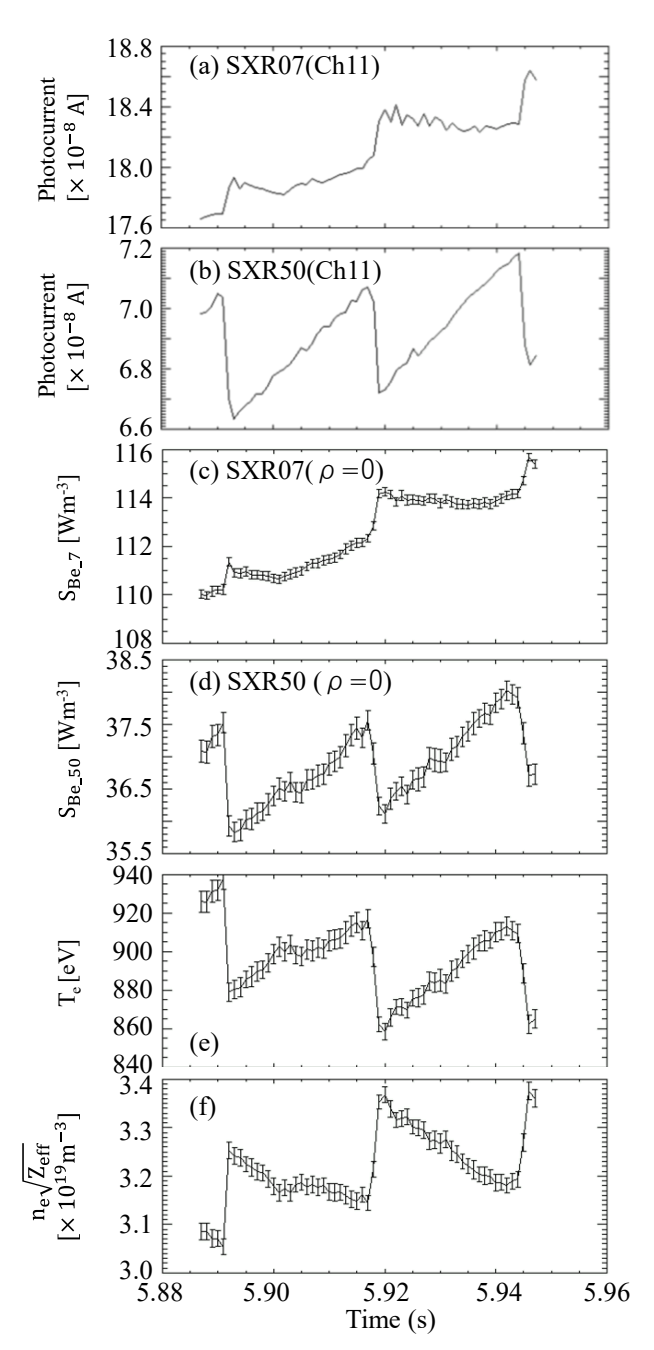


Figure 4 Time traces of (a)photocurrent of SXR07 and (b)SXR50, (c)reconstructed local emission power density of SXR07 and (d)SXR50, (e)local electron temperature, and (f)local  $n_e\sqrt{Z_{eff}}$ . (c)(d)(e)(f) are parameters at the plasma centre. Error bar indicates the uncertainty by shot noise and background noise of the soft x-ray diagnostic system.

To investigate the plasma parameter profile during the core sawtooth, analyses using the soft x-ray diagnostic system were performed.

#### RESULTS

Figure 3 shows time traces of a helium plasma discharge having the core sawtooth. In this discharge, the flat top of the plasma current is from around 2 to 6 seconds with divertor configuration without EC heating. The core sawtooth is observed from 5 to the end of discharge. The peak of soft x-ray emission and sawtooth oscillation is along channel 11. The line electron density is gradually increasing during the flat top phase.

Figure 4 (a) and (b) show transient changes of photocurrent of SXR07 and SXR50 along channel 11 with a period of a sawtooth oscillation. Photocurrent of SXR07 and SXR50 increases and decreases, respectively, at 5.917 seconds, which is a timing of sawtooth crash. It indicated that the oscillation direction for SXR07 and SXR50 are opposite. Figure 4 (c) and (d) show local emission power density, S<sub>Be\_7</sub>, and, S<sub>Be 50</sub>, at the plasma centre which are reconstructed by the Abel reconstruction. The opposite oscillation is also obtained in the local emission power density. It is indicated that the opposite oscillation does not appear by effect of line-integration along each sightline. The absolute intensity of the oscillation for SXR07 and SXR50 are comparable despite the three times larger emission power density of SXR07 than SXR50. The electron temperature at the plasma centre decreases at the sawtooth crash, as shown in Figure 4(e). The time trace of the electron temperature is similar to SXR50. From (1),the  $S_{Be_{-7}}$  $S_{Be\ 50}$ monotonically increase with increasing the electron temperature. The opposite oscillation and the comparable absolute oscillation intensity are not obtained by only the oscillation of the electron temperature. Figure 4(f) shows that the product of electron density and square root of effective charge,  $n_e \sqrt{Z_{eff}}$ , suddenly increases at sawtooth crash at the plasma centre and decreases by the next sawtooth crash. It indicates that the opposite oscillation of SXR07 and SXR50 is obtained by the opposite oscillation between the electron temperature and  $n_{e}\sqrt{Z_{eff}}$ . The

oscillation intensities of each plasma parameter at the plasma centre are about 2%, 4%, 7%, and 6% for  $S_{Be\_7}$ ,  $S_{Be\_50}$ ,  $T_e$ , and  $n_e\sqrt{Z_{eff}}$ , respectively.

# 4. DUSCUSSIONS

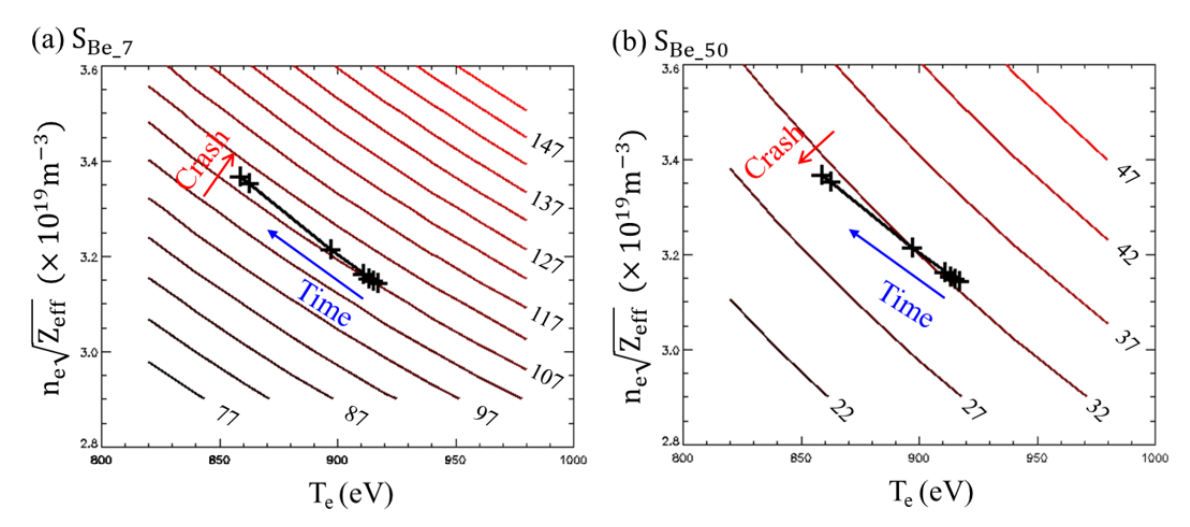


Figure 5 Dependences of the local emission power density of (a)SXR07 and (b)SXR50 on the electron temperature and  $n_e\sqrt{Z_{eff}}$ . Thick lines and numerical characters in graph indicate contours for the emission power density. Cross symbols and black line indicate plasma parameter changes from 3ms before to 3ms after sawtooth crash. (5.914-5.920 s)

Thick lines in figure 5 show the dependence of the  $S_{Be\_7}$  and  $S_{Be\_50}$  on the electron temperature and  $n_e\sqrt{Z_{eff}}$  using a contour. The cross symbols and a black line indicate plasma parameter changes at the plasma centre for the sawtooth crash from 5.194 s to 5.920 s. In this figure, in the case that the cross symbol and black line cross the thick line,  $S_{Be\_7}$  or  $S_{Be\_50}$  oscillates at a sawtooth crash. Oscillation direction is determined by the crossing direction. In figure 5 (a), black lines cross contour lines from the low power density side at each sawtooth crash, leading to the  $S_{Be\_7}$  increase at the sawtooth crash. On the other hand, the black line crosses the contour lines of

S<sub>Be50</sub> from the high power density side, leading to the  $S_{Be\ 50}$ decrease. Furthermore, the oscillation intensities of  $S_{Be_{2}}$  and  $S_{Be_{2}}$  are determined by the angle between contour lines and the black line. In this discharge, because the contour lines of S<sub>Be\_7</sub> is closer to parallel to the black line than the contour lines of  $S_{Be\ 50}$ , the oscillation of  $S_{Be\_7}$  is suppressed. Therefore, the opposite oscillation and comparable oscillation intensity of  $S_{Be07}$ and S<sub>Be50</sub> can be explained by the relation between the contour and the changes of the electron temperature and  $n_e \sqrt{Z_{eff}}$ . Because the inclination of both  $S_{Be07}$  and  $S_{Be50}$ contour is flattened at higher electron temperatures, in the case that the electron temperature, the opposite oscillation of  $S_{Be07}$  and  $S_{Be50}$  is expected to disappear.

Figure 6 (c) shows the spatial profile of the electron temperature 3 ms before and after a sawtooth crash with the normalized minor radius,  $\rho$ . In these time slices, the electron temperature at the plasma centre is about 1 keV. The change direction of the electron temperature at the sawtooth crash is different according to the inside and outside

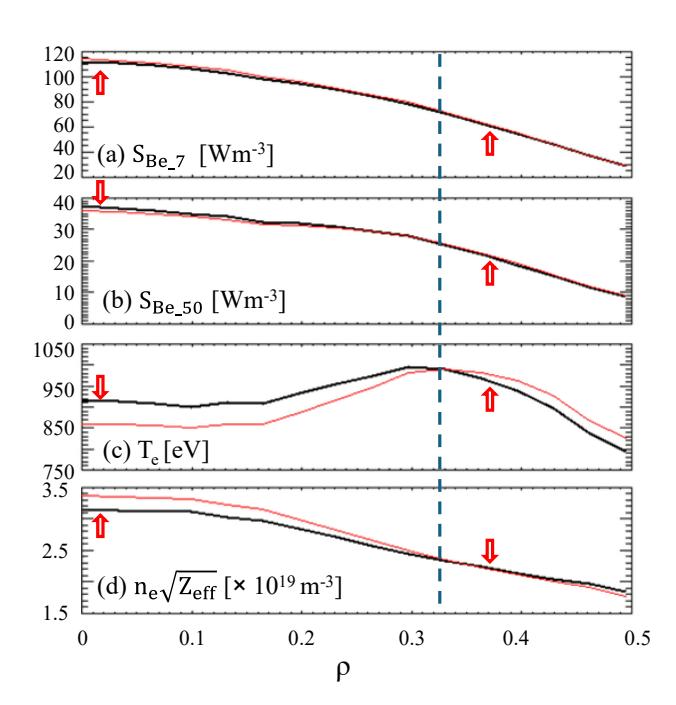


Figure 6 Spatial profiles of local emission power density reconstructed from (a) SXR07 and (b)SXR50, (c) electron temperature, and (d)  $n_e\sqrt{Z_{eff}}$  3ms (black) before and (red) after sawtooth crash. Dashed blue line indicates the inversion radius. Red arrows indicate change directions.

6

4

of  $\rho = 0.32 - 0.34$ . It indicates the inversion radius of the electron temperature. Figure 6 (a) and (b) shows the spatial profiles of  $S_{Be_{-}7}$  and  $S_{Be_{-}50}$ . Both emission profiles are peaked at the plasma centre.  $S_{\mbox{\footnotesize{Be}}_{\mbox{\footnotesize{-}}7}}$  increases at both the inside and outside of the inversion radius of the electron temperature. On the other hand, S<sub>Be 50</sub> increases and decreases at the inside and outside of the inversion radius, respectively. The change is similar to that of the electron temperature. The  $n_e \sqrt{Z_{eff}}$  shows the opposite change direction with the electron temperature at both of the inside and outside of the inversion radius as shown in Figure 6

Brightness (×10<sup>15</sup> ph/sr m² s nm) 0 6 Time (s) Figure 7 A time trace of (black) measured visible bremsstrahlung

Vis. Brem.(by Spec.)

Synthetic (by SX)

emission and (red) synthetic visible bremsstrahlung emission evaluated by the soft x-ray diagnostic system (#E101008). Error bar means the statistical error by background and shot noises.

The validity of the profiles of the plasma parameters in figure 6 is investigated with a comparison between bremsstrahlung emission intensity taken by a visible spectrometer, which views in a tangential direction, with that taken by the soft x-ray diagnostic system, which views on a poloidal cross section using a synthetic signal scheme as shown in Figure 7. The measured visible bremsstrahlung emission and the

synthetic signal are consistent within statistical error, showing the absolute emission power density profiles evaluated by the soft x-ray diagnostic system, shown in Figure 6, are valid in terms of uncertainty quantification.

The same analyses with figure 6 were performed on 36 sawtooth crashes in the core sawtooth phase (5.1 - 6.0 s). Figure 8 shows differences of plasma parameter profile between after and before the sawtooth crash. Except the outside of  $\rho = 0.6$  which has a weak signal level, change directions of each profile at the sawtooth crash is different beyond the uncertainty of multiple sawtooth crashes. In the core sawtooth phase,  $S_{Be\ 7}$ increases at sawtooth crashes regardless of whether it's inside or outside of the inversion radius. S<sub>Be 50</sub> and the electron temperature decrease at the inside of the inversion radius and increase at the outside.  $n_e \sqrt{Z_{eff}}$ increase at the centre of the plasma and decrease at the outside of the inversion radius. This result indicates an inflow of the electron or/and impurity across the inversion radius. Differences of S<sub>Be 50</sub> and the electron temperature at  $\rho = 0.45$  are about 60% of values at  $\rho = 0.0$ . On the other hand, differences of  $n_e\sqrt{Z_{eff}}$  at  $\rho=0.45$  is about 35 % of the centre of the plasma. The smaller difference of  $n_e \sqrt{Z_{eff}}$  at the  $\rho =$ 0.45 than the plasma centre can be explained

with continuity of total  $n_e \sqrt{Z_{eff}}$ . With the plasma volume,  $V(\rho)$ , the intensity of the

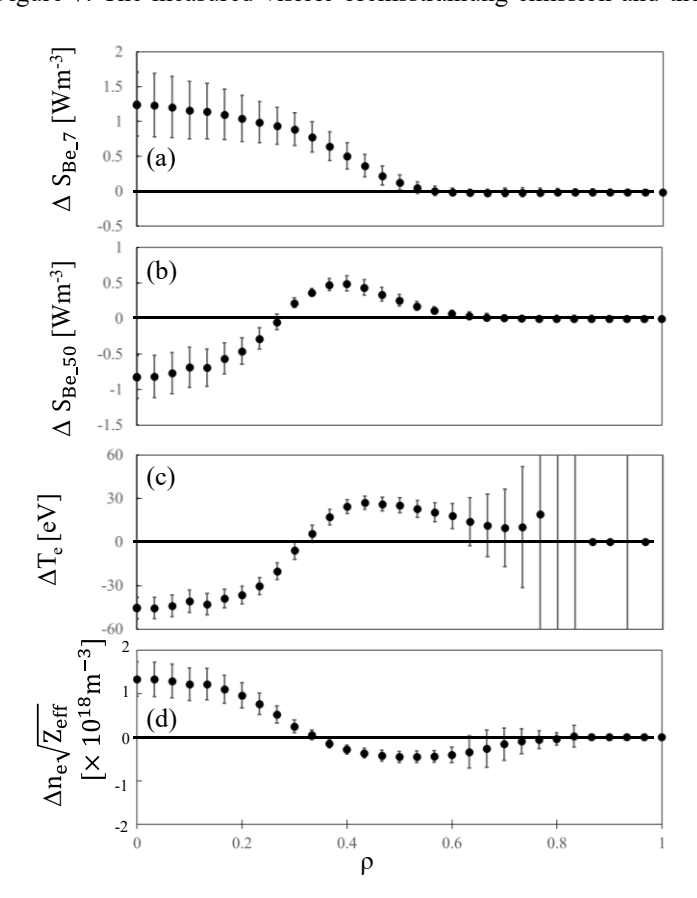


Figure 8 spatial profiles of difference of (a) local emission power density of SXR07 and (b)SXR50, and (c)electron temperature, and  $n_e\sqrt{Z_{eff}}$  from before crash to after crash. Error bars are standard deviations of 36 sawtooth crashes in 5.1 - 6.0 s. (#101008)

inflow of electron or/and impurity,  $\Gamma_e$ , is expressed as

$$\Gamma_{e} = \int \Delta n_{e} \sqrt{Z_{eff}}(\rho) \ V(\rho) d\rho. \ (3)$$

In the case of that  $Z_{eff}$  is constant,  $\Gamma_{\!e}$ means that the total increased/decreased number of electrons in a specific region. Figure 9 shows  $\Gamma_e$  of the inside ( $\rho = 0$  – 0.34) and the outside ( $\rho = 0.34 - 0.6$ ) of the inversion radius. The region of the outside of ( $\rho = 0.6$ ) is not included in this evaluation due to large error bar in figure 8(d). In the case that a constant Z<sub>eff</sub> is assumed,  $\Gamma_{e}$  of the inside means an increased number of electrons by inflow across the inversion radius.  $\Gamma_e$  of the outside means the decreased number of electrons by flow across the inversion radius or  $\rho = 0.6$  boundary.  $\Gamma_e$  of the inside and the outside are comparable at each sawtooth crash. It indicates that the

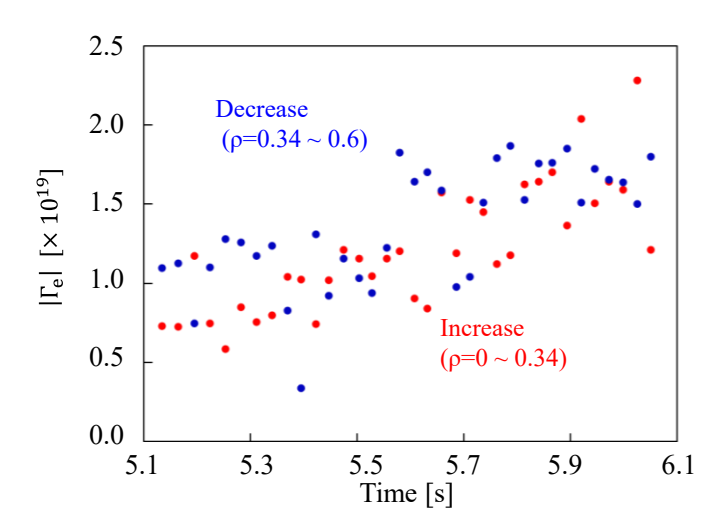


Figure 9 (red) Total increase of  $n_e\sqrt{Z_{eff}}$  at the inside of the inversion radius ( $\rho=0.0\sim0.34$ ) for each sawtooth crash. (blue) Total decrease of  $n_e\sqrt{Z_{eff}}$  at the outside of the inversion radius ( $\rho=0.34\sim0.6$ ). Horizontal axis is time of sawtooth crash occurred.

inflow intensity evaluated from the inside and outside is not inconsistent.  $\Gamma_e$  of the inside of the inversion radius is  $0.4-2.1\times 10^{19}$  and shows an increasing trend with increasing the line integrated density in the figure 3.  $\Gamma_e$  in figure 9 are around 1 - 2% of the total number of electrons in plasma volumes from  $\rho=0.0$  to  $\rho=0.6$ . The  $\Gamma_e$  is not significantly large compared to the total number of electrons or impurities in the whole plasma volume in this discharge. However, because  $\Gamma_e$  increases with increasing the line electron density, it is necessary to investigate the dependence of the  $\Gamma_e$  on plasma parameter in the next experimental campaign. Furthermore, because the effects of electrons and impurities cannot be separated in this analysis, the main component of  $\Gamma_e$  is still required to investigate.

# SUMMARY

Using the power spectrum of bremsstrahlung, which was evaluated by the soft x-ray diagnostic system, evolutions of plasma parameter profiles were evaluated in core sawtooth oscillation in JT-60SA integrated commissioning phase. The evaluation indicates that the observed opposite phase oscillations between high-energy and low-energy soft x-ray bremsstrahlung emissions are due to opposite changes in the electron temperature and density or effective charge. From the analysis of profiles of the electron temperature and the product of the electron density and the effective charge, a possible inflow of electrons and/or impurities across the inversion radius at the sawtooth crash is indicated.

# **ACKNOWLEDGEMENTS**

JT-60SA was jointly constructed and is jointly funded and exploited under the Broader Approach Agreement between Japan and EURATOM.

#### REFERENCES

- [1] T Bando, T Wakatsuki, M Honda, A Isayama, K Shinohara, S Inoue, M Yoshida, G Matsunaga, M Takechi, N Oyama, S Ide, Effect of m/n = 2/1 neoclassical tearing mode on sawtooth collapse in JT-60U, Plasma Phys. Control. Fusion, 63 (2021) 085009
- [2] Y. Nagayama et. al., Sawtooth Oscillation in Current-Carrying Plasma in the Large Helical Device, Phys. Rev. Lett. 90, (2003) 205001

#### IAEA-CN-316/2793

- [3] E. Westerhof, P. Smeulders, N.J. Lopes Cardozo, Observations of sawtooth postcursor oscillations in JET and their bearing on the nature of the sawtooth collapse, Nuclear Fusion, **29** (1989) 1056
- [4] M. Yamada, F. M. Levinton, N. Pomphrey, R. Budny, J. Manickam, Y. Nagayama, Investigation of magnetic reconnection during a sawtooth crash in a high-temperature tokamak plasma, Phys. Plasmas 1 (1994) 3269–3276
- [5] M. Zanini, B. Buttenschön, H.P. Laqua, H. Thomsen, T. Stange, C. Brandt, H. Braune, K.J. Brunner, A. Dinklage, Y. Gao, M. Hirsch, U. Höfel, J. Knauer, S. Marsen, N. Marushchenko, A. Pavone, K. Rahbarnia, J. Schilling, Y. Turkin, R.C.Wolfl, A. Zocco and the W7-X Team, Confinement degradation and plasma loss induced by strong sawtooth crashes at W7-X. Nucl. Fusion 61 (2021) 116053
- [6] I. Furno, H. Weisen, TCV team, Observation of inward and outward particle convection in the core of electron cyclotron heated and current driven plasmas in the Tokamak à Configuration Variable, Phys. Plasmas 10 (2003) 2422–2428
- [7] Y. Yamashita, Abel-inversion by Wiener filter, JAERI-Memo, JAERI 87-206 (1987)
- [8] R. Sano, H. Homma, M. Takechi, T. Nakano, Soft x-ray diagnostics system for electron temperature measurement in the integrated commissioning phase of JT-60SA, Rev. Sci. Instrum. 95 (2024) 073532
- [9] T. P. Donaldson, Theory of foil-absorption techniques for plasma X-ray continuum measurements, Plasma Phys. **20**, 1279 (1978).